Sulfur Dehydrogenase of *Paracoccus pantotrophus*: The Heme-2 Domain of the Molybdoprotein Cytochrome *c* Complex Is Dispensable for Catalytic Activity†

Frank Bardischewsky,‡,§ Armin Quentmeier,‡,§ Dagmar Rother,§ Petra Hellwig,|| Susanne Kostka,⊥ and Cornelius G. Friedrich*,§

Lehrstuhl für Technische Mikrobiologie, Fachbereich Bio- und Chemieingenieurwesen, Universität Dortmund, Emil-Figge-Strasse 66, D-44221 Dortmund, Germany, Institut für Biophysik, J. W.-Goethe-Universität, Theodor-Stern-Kai 7 Haus 75, 60590 Frankfurt am Main, Germany, and Max-Delbrück-Centrum für Molekulare Medizin, D-13122 Berlin, Germany

Received December 20, 2004; Revised Manuscript Received March 14, 2005

ABSTRACT: Sulfur dehydrogenase, $Sox(CD)_2$, is an essential part of the sulfur-oxidizing enzyme system of the chemotrophic bacterium *Paracoccus pantotrophus*. $Sox(CD)_2$ is a $\alpha_2\beta_2$ complex composed of the molybdoprotein SoxC (43 442 Da) and the hybrid diheme *c*-type cytochrome SoxD (37 637 Da). $Sox(CD)_2$ catalyzes the oxidation of protein-bound sulfur to sulfate with a unique six-electron transfer. Amino acid sequence analysis identified the heme-1 domain of SoxD proteins to be specific for sulfur dehydrogenases and to contain a novel ProCysMetXaaAspCys motif, while the heme-2 domain is related to various cytochromes c_2. Purification of sulfur dehydrogenase without protease inhibitor yielded a dimeric $SoxCD_1$ complex consisting of SoxC and $SoxD_1$ of 30 kDa, which contained only the heme-1 domain. The heme-2 domain was isolated as a new cytochrome $SoxD_2$ of about 13 kDa. Both hemes of SoxD in $Sox(CD)_2$ are redox-active with midpoint potentials at $E_{m_1} = 218 \pm 10$ mV and $E_{m_2} = 268 \pm 10$ mV, while $SoxCD_1$ and $SoxD_2$ both exhibit a midpoint potential of $E_m = 278 \pm 10$ mV. Electrochemically induced FTIR difference spectra of $Sox(CD)_2$, $SoxCD_1$, and $SoxD_2$ were distinct. A carboxy group is protonated upon reduction of the $SoxD_1$ heme but not for $SoxD_2$. The specific activity of $SoxCD_1$ and $Sox(CD)_2$ was identical as was the yield of electrons with thiosulfate in the reconstituted Sox enzyme system. To examine the physiological significance of the heme-2 domain, a mutant was constructed that was deleted for the heme-2 domain, which produced $SoxCD_1$ and transferred electrons from thiosulfate to oxygen. These data demonstrated the crucial role of the heme-1 domain of SoxD for catalytic activity, electron yield, and transfer of the electrons to the cytoplasmic membrane, while the heme-2 domain mediated the $\alpha_2\beta_2$ tetrameric structure of sulfur dehydrogenase.

The molybdoprotein diheme cytochrome *c* complex sulfur dehydrogenase, $Sox(CD)_2$, is part of the sulfur-oxidizing enzyme system of the aerobic chemotrophic bacterium *Paracoccus pantotrophus* (eq 1; *1*). The oxidation of reduced inorganic sulfur compounds to sulfuric acid (Sox) represents one-half of the global sulfur cycle, which is primarily mediated by aerobic chemotrophic bacteria and archaea and anaerobic phototrophic bacteria (*2*−*8*).

The *sox* genetic determinants and their gene products have been characterized from *P. pantotrophus* (*8*−*10*). The sulfur-oxidizing enzyme system of *P. pantotrophus* is reconstituted from four periplasmic proteins, SoxYZ, SoxXA, $Sox(CD)_2$, and SoxB, which together catalyze the oxidation of hydrogen sulfide, sulfur, thiosulfate, and sulfite with horse cytochrome *c* as a final electron acceptor. $Sox(CD)_2$ is not required for sulfite oxidation, and each of the proteins alone is inactive with either substrate (*1*, *11*). The current model proposes thiosulfate to be linked to the sulfhydryl group of the invariant cysteine-138 residue of the SoxY subunit of the SoxYZ complex by the heterodimeric heme enzyme SoxXA to yield thiocysteine-*S*-sulfate (*8*, *12*, *13*). The outer sulfate is proposed to be hydrolyzed off by the monomeric dimanganese SoxB protein to yield cysteine persulfide and sulfate. The outer sulfur atom of cysteine persulfide is oxidized to cysteine-*S*-sulfate by $Sox(CD)_2$ (eq 2). Finally, sulfate is again hydrolyzed off by the SoxB protein to regenerate SoxY (*8*) (Figure 1). The Sox enzyme system yields 8 mol of electrons/mol of thiosulfate, and omission of $Sox(CD)_2$ from reconstitution of the enzyme system reduces the yield to two electrons. Thus, $Sox(CD)_2$ mediates a unique six-electron transfer and was designated sulfur dehydrogenase (eq 2) (*1*).

$$HS{-}SO_3H + 5H_2O + 8\text{cyt } c_{ox} \rightarrow 2H_2SO_4 + 8\text{cyt } c_{red} + 10H^+ \quad (1)$$

$$SoxY{-}S{-}SH + 3H_2O + 6\text{cyt } c_{ox}\ Sox(CD)_2 \rightarrow SoxY{-}S{-}SO_3H + 6\text{cyt } c_{red} + 6H^+ \quad (2)$$

Sulfur dehydrogenase is a $\alpha_2\beta_2$ heterotetrameric complex of 180 kDa with the molybdenum cofactor containing subunit SoxC (43 442 Da) and the diheme *c*-type cytochrome subunit

† Financial support from the DFG to C.G.F. (Fr 318/8-1) is gratefully acknowledged.

* To whom correspondence should be addressed. Telephone: +49-231-755-5115. Fax: +49-231-755-5118. E-mail: cornelius.friedrich@udo.edu.

‡ These authors contributed equally to this study.

§ Universität Dortmund.

|| J. W.-Goethe-Universität.

⊥ Max-Delbrück-Centrum für Molekulare Medizin.

10.1021/bi047334b CCC: $30.25
Published on Web 04/08/2005

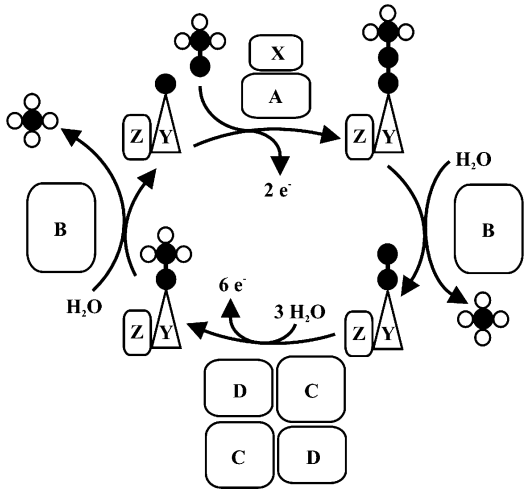

FIGURE 1: Model of protein-bound oxidation of thiosulfate to sulfate in *P. pantotrophus* (*8*, with permission). The capital letters indicate the Sox proteins according to their gene designation. X and A, Cytochrome complex SoxXA; B, dimanganese protein SoxB; C and D, heterotetrameric molybdoprotein−cytochrome *c* complex $Sox(CD)_2$. Black circles indicate sulfur atoms, and white circles indicate oxygen atoms.

SoxD (37 637 Da) (*14*). SoxC (430 amino acids) is about 30% identical to sulfite oxidases in overlaps of 264−326 amino acids but phylogenetically clearly distinct (*8*, *15*). Sulfite oxidases of eukaryotic sources are monomeric molybdoprotein−heme enzymes, which harbor the molybdenum cofactor and a b_5 heme moiety on one polypeptide (*16*). Sulfite oxidase from the chemotrophic sulfur bacterium *Starkeya novella* is a heterodimeric complex of a molybdoprotein and a *c*-type cytochrome encoded by the *sorAB* genes, which are located separately from the *sox* gene cluster. This bacterium harbors also the *soxCD* genes for sulfur dehydrogenase, which are located within the *sox* gene cluster (*16*, *17*). *S. novella* cells oxidize sulfite (*16*), while *P. pantotrophus* cells are unable to do so (*18*, *19*). In summary, sulfur dehydrogenase of *P. pantotrophus* differs significantly from sulfite oxidases of eukaryotic and other prokaryotic sources with respect to the catalytic reaction, size, heme content, and primary and quaternary structure.

SoxD of *P. pantotrophus* is a periplasmic hybrid cytochrome of 384 amino acids with two heme domains. Previous analyses characterized the matured SoxD (360 amino acids) as a class I *c*-type cytochrome with no significant homology of the heme-1 domain (amino acid 25−220) to other cytochromes, while the heme-2 domain (amino acid 256−384) is 39−54% identical to cytochromes c_2 with various functions in chemo- and phototrophic bacteria (*15*). Both heme domains are linked by a proline-alanine-rich intervening sequence of about 35 amino acids. The significance of each of the two heme domains of SoxD in $Sox(CD)_2$ for catalytic activity or electron transfer is not known (*15*).

We here report that the heme-1 domain of SoxD is exclusively present in sulfur dehydrogenases of sulfur oxidizing proteobacteria and contains a novel SoxD-specific motif. A dimeric molybdoprotein−monoheme cytochrome complex $SoxCD_1$ was isolated from extracts of the wild-type *P. pantotrophus* that contains just the heme-1 domain of SoxD, $SoxD_1$. We have constructed a mutant producing the $SoxCD_1$ complex and demonstrate that $Sox(CD)_2$ and $SoxCD_1$ were identically active *in vitro*. This is the first report that deletion of a complete heme domain of a cytochrome did not affect the catalytic but the structural properties of an enzyme.

MATERIALS AND METHODS

Strains, Plasmids, and Growth Conditions. P. pantotrophus $GB17^T$ (*9*), strain GBΩX, and plasmids used in this study are listed in Table 1. These strains and *Escherichia coli* strains were cultivated aerobically at 30 °C. The conditions for chemotrophic growth of *P. pantotrophus* strains with thiosulfate, mixotrophic growth with succinate and thiosulfate, cell harvest, and storage at −20 °C were identical as described previously (*14*).

Purification of $Sox(CD)_2$, $SoxCD_1$, and $SoxD_2$. Extracts of cells were obtained from thawed cells by French pressure treatment, differential centrifugation, and ammonium sulfate fractionation. Soluble proteins precipitating between 44 and 65% ammonium sulfate saturation were redissolved and referred to as cell-free extracts and used for determination of initial enzyme activities (*14*). Sulfur dehydrogenase, either $Sox(CD)_2$ or $SoxCD_1$, was purified to homogeneity from extracts of *P. pantotrophus* GB17 cultivated with thiosulfate (*14*), wherefrom also SoxYZ, SoxB, and SoxXA were purified to homogeneity after several chromatographic steps (*11*).

The $SoxCD_1$ complex from *P. pantotrophus* GBΩX-(pVKP6; pRI*soxCD*$_1$) was purified from cells cultivated mixotrophically, and the purification procedure was identical as for the $Sox(CD)_2$ complex (*14*). The purification of the heme-2 domain of SoxD, $SoxD_2$, from extracts of the wild type comprised identical steps as $SoxCD_1$ involving chromatography on Q-Sepharose, gel filtration on Sephadex G-200, and anion exchange on Resource Q (*14*).

The total heme content was determined by the pyridine hemochrome method (*20*).

The activity of $Sox(CD)_2$ and $SoxCD_1$ was examined from the reconstituted thiosulfate-oxidizing enzyme system using either 0.50 μM of $Sox(CD)_2$ or 1.0 μM of $SoxCD_1$ and 0.50 μM of SoxXA, SoxYZ, and SoxB with 70 μM horse cytochrome *c* as described (*14*). The DNA sequence of *soxCD* and of other genes from the *sox* gene region of *P. pantotrophus* is accessible at the EMBL data library under accession number X79242 PDSOX.

Electrochemical Measurements. The ultrathin layer spectroelectrochemical cell for the UV−vis and IR detection was described previously (*21*). The gold grid working electrode was chemically modified with a 1:1 mixture of 2 mM cysteamine and 2 mM mercaptopropionic acid in aqueous solution. To accelerate the redox reaction, 15 different mediators were added to a final concentration of 45 μM each as detailed in ref *22*. Potentials quoted with the data have been obtained with a Ag/AgCl/3 M KCl reference electrode and +208 mV added for SHE′ (pH 7) values. All measurements were performed at 5 °C.

Reaction-Induced FTIR Difference Spectroscopy. FTIR difference spectra as a function of the applied potential were obtained with a modified IFS 25 (Bruker, Germany) for the 2000−1000 cm^{-1} range. In all experiments, the protein solution was first equilibrated at the initial potential of the electrode and single-beam spectra in the IR range were recorded. Then, a potential step toward the final potential

Table 1: Bacterial Strains and Plasmids[a]

strain or plasmid	relevant genotype or phenotype	reference or source
Escherichia coli		
S17-1	*recA pro thi hsdS*, RP4-*tra*-functions *supE44*	*34*
Paracoccus pantotrophus		
GB17	Sox^+	*9, 10*
GBΩX	Sox^-	this paper
GB*soxF*Δ	Sox^+ *soxF*Δ	*1*
plasmids		
pJOE733.2	Ap^r, lacZa′, positive selection vector	*36*
pSUP202	Cm^r, Tc^r, Tra^-, Mob^+	*34*
pHP45Ω-Km	Ap^r, Km^r	*47*
pBSP3.4	3.4-kb *Sal*I−*Pst*I *sox*-DNA fragment in pBluescript SK^-	*33*
pVK101	Km^r, Tc^r, Tra^-, Mob^+	*48*
pRI1	Cm^r, Sm^r	*35*
pSSP3.4ΩX	pSUP202 containing the 3.4-kb insert of pBSP3.4 with the Ω-Km fragment of pHP45Ω-Km integrated in *soxX*	this paper
pVKB9	8851-bp *Bam*HI fragment *soxR*′−*soxE*′ in pJOE773.2	*1*
pJOEE9	9494-bp *Eco*RI fragment of pEG12 in pJOE733.2	this paper
pJOEP6	5953-bp *Pst*I fragment of pJOEE9 with the *soxVWXYZAB* genes in pJOE733.2	this paper
pVKP6	5977-bp *Hin*dIII fragment of pJOEP6 in pVK101	this paper
pRI*soxCD*$_1$	2118-bp *Bam*HI- and *Xho*I-restricted PCR fragment with *soxCD*$_1$ in pRI1	this paper
pEG12	13-kb Sox-relevant DNA in pSUP202	*49*
pUC19	Ap^r*lacZ*α	*37*
pRD146	1250-bp fragment containing *soxD* in pUC19	this paper

[a] Sox, chemotrophic growth with thiosulfate.

was applied, and the single-beam spectrum of this state was again recorded after equilibration. Subsequently, difference spectra, as presented in this work, were calculated from the two single-beam spectra with the initial single-beam spectrum taken as the reference. No smoothing or deconvolution procedures were applied. The equilibration at the applied potential in the range from −0.15 to 0.4 V generally took less than 3 min. Equilibration times were determined by monitoring FTIR difference spectra of the same sample, by measuring double difference spectra until no more changes could be detected. Typically, 128 interferograms at 4 cm^{-1} resolution were co-added for each single-beam IR spectrum and Fourier-transformed using triangular apodization, and 5−10 difference spectra were usually averaged. The noise level in the difference spectra was estimated to be around $30-50 \times 10^{-6}$ absorbance units in the spectral range under consideration, except for the region of the strongly absorbing water bending and protein amide I modes at ca. 1650 cm^{-1}, where the noise was slightly higher.

Spectroscopic Techniques. Electronic absorption and difference spectra were recorded with a Shimadzu UV160A spectrophotometer with a 1 cm light path.

Protein Analytical Techniques. The molecular masses of denatured proteins were determined by SDS−PAGE according to Laemmli (*23*) and of native proteins by density-gradient gel electrophoresis (DGGE) according to Andersson et al. (*24*). Proteins were stained with Coomassie blue (*25*), and stain intensities from SDS−PAGE, DGGE, or immunoblot analysis were quantified by the Scion image software package. Molecular masses of proteins were also determined by matrix-assisted laser desorption ionization (TofSpec2E, Micromass, Manchester, U.K.).

N-Terminal amino acid sequences were determined from blots of denatured pure proteins. The membrane carrying the protein species was cut out and subjected to automated Edman degradation using a protein sequencer system model 494A/190A (Applied Biosystems, Foster City, CA) (*26*).

Immunoblot analysis (*27*) was done according to the "semidry" procedure using the multiphor electrophoretic system (Pharmacia, Freiburg, Germany). Antibodies against the oligopeptides VESREETSKYTDLM (OP-C), FYPDDR-DQTEYPLF (OP-D_1), and KMSFAGLKKEDERA (OP-D_2), detected SoxC, $SoxD_1$, and $SoxD_2$ antigens, respectively.

Protein from cell-free extracts and homogeneous enzymes was determined according to Bradford (*28*).

DNA Techniques. Standard DNA techniques were applied (*29*). Plasmids were prepared in small scale from *E. coli* as described by Kieser (*30*). Genomic DNA was isolated according to Ausubel et al. (*31*). For DNA sequencing, DNA was prepared with the High Pure plasmid isolation kit (Boehringer, Mannheim, Germany).

Construction of P. pantotrophus GBΩX. The *soxX* gene was disrupted by inserting the Ω-Km interposon of pHP45Ω-Km (*32*) by gene replacement using the suicide plasmid pSSP3.4ΩX. This plasmid was constructed from plasmid pBSP3.4, a $pBSK^-$ (Stratagene) derivative with a 3.4-kb *Sal*I−*Pst*I DNA insert containing *soxX* (*33*). The Ω-Km fragment was isolated from pHP45Ω-Km by *Bam*HI restriction, and the fragment was treated with mung bean nuclease to obtain blunt ends. This fragment was cloned into the *Bal*I site of pBSP3.4, which was located within the *soxX* gene resulting in pBSP3.4ΩX. The insert carrying the Ω-Km interposon was isolated from pBSP3.4ΩX, restricted with *Xba*I and *Xho*I, and treated with mung bean nuclease. The fragment was then cloned into the *Eco*RV site of pSUP202 (*34*) resulting in plasmid pSSP3.4ΩX. Plasmid pSSP3.4ΩX was transformed into *E. coli* S17-1 (*34*) and conjugated into *P. pantotrophus* GB17. Heterogenote transconjugants were selected exhibiting the Km^r and Cm^r phenotype. To obtain the homogenote strain with a *soxX*::Ω insertion, one single (Km^r, Cm^r) colony was cultivated with shaking for 3 days in mineral medium containing 20 mM sodium succinate. About 10^3 cells were plated on mineral agar containing 300 μg Km/mL. To verify the integration of the Ω-Km fragment into the chromosomal DNA of *P. pantotrophus*, colonies

exhibiting the (Km^r, Cm^s) phenotype were analyzed by colony hybridization using pSUP202 labeled with digoxigenin (DIG; Boehringer) and the DIG-labeled Ω-Km fragment as probes. One clone gave a signal with the Ω-Km probe but not with the pSUP202 probe, which was designated strain GBΩX and was used as a background for production of the $SoxCD_1$ complex.

Construction of Plasmid pRIsoxCD₁. The expression of *soxCD₁* in *P. pantotrophus* required several cloning steps. Chromosomal DNA comprising the complete *soxC* gene and that encoding *soxD₁* was amplified by PCR using primer FB-C, 5′-CCAACACctcgagCACCGTGACCGGGGTCTGAC-3′, and primer FB-D, 5′-GTGGTCAAGGCCGCCTGAATG-GCGCCggatccC-3′. The primers were designed to give FB-C an *Xho*I and FB-D a *Bam*HI restriction site, indicated in lowercase letters. In addition, an TGA codon was integrated into primer FB-D, leading to a stop of translation after amino acid alanine[261]. The amplified DNA was restricted with *Bam*HI and *Xho*I and cloned into plasmid pRI1 (*35*) to yield the 8792-bp pRI*soxCD₁*.

The *sox* structural genes *soxYZ*, *soxXA*, and *soxB* were expressed from the hybrid plasmid pVKP6. The 9494-bp *Eco*RI fragment of pEG12 was cloned into *Eco*RI-restricted vector pJOE733.2 (*36*) to yield plasmid pJOEE9. *Pst*I restriction of pJOEE9 yielded a 5953-bp fragment which contained the *soxVWXYZAB* genes. This fragment was cloned into vector pJOE733.2 to yield pJOEP6. Therefore, the *sox*-relevant DNA region was isolated by restriction with *Hin*dIII and cloned into the broad host range vector pVK101. The resulting plasmid pVKP6 was used for expression of the *soxXYZAB* genes.

DNA Sequence Analysis of Mutant GBsoxFΔ. The DNA sequence of the mutant GB*soxF*Δ was analyzed with respect to the upstream chromosome junction of the fragment carrying the deletion in *soxF*. DNA of the wild type and strain GB*soxF*Δ was used as a template for PCR. The DNA was amplified with primer S27, 5′-AAAAGGATCCTAT-CACAACAACGGCAT-3′, and primer S28, 5′-TTTTAAGCT-TACAGGAGTTTGCGCTGT-3′, which introduced a restriction site for *Bam*HI in S27 and for *Hin*dIII in S28 (underlined). As expected, both PCR assays yielded products of 1250 bp. Two PCR assays with *soxD* from GB*soxF*Δ were purified (NucleoSpin Extract, Machery-Nagel) and combined. The fragments were restricted with *Bam*HI and *Hin*dIII purified and cloned into pUC19 (37) restricted by the same enzymes to yield the pRD146 plasmid series. For sequence analysis, the following primers were used: universal primer 5′-IRD-800-AGG GTT TTC CCA GTC ACG ACG TT-3′, reverse primer 5′-IRD-800-AAA CAG CTA TGA CCA TGA TTA CGC C-3′, and primer S29 5′-IRD-800-ACG ACG GCG ACC AGA CCG AAT AT-3′.

RESULTS AND DISCUSSION

Sequence Analysis. Amino acid sequence analysis revealed that the primary structure of SoxC of *P. pantotrophus* is distinct from that of sulfite oxidases (*15*), and kinetic data with $Sox(CD)_2$ confirmed this analysis (*8*). SoxD is a diheme hybrid cytochrome composed of the heme-1 and heme-2 domains. Alignments of the primary structure of SoxD of *P. pantotrophus* revealed that exclusively the heme-1 domain, designated $SoxD_1$, was encoded by the respective genes in sulfur-oxidizing bacteria and that these genes were located within their *sox* gene clusters. The heme-2 domain is not special to SoxD of *P. pantotrophus* and has also been detected in SoxD of *Silicibacter pomeroyi* (accession AAV94303) and in SoxD of the chemotroph *Pseudaminobacter salicylatoxidans* (TrEMBL accession Q5ZQM8), where the heme-2 domain is located at the N terminus, while the heme-1 domain is at the C terminus. As in *P. pantotrophus* both heme domains are linked by an alanine-proline-rich intervening sequence (data not shown). The heme-2 domain, however, is not present in the respective protein of the chemotroph *Starkeya novella* (accession AAF61450), the dinitrogen-fixing bacterium *Bradyrhizobium japonicum* (accession BAC48782, *38*), the methylotroph *Methylobacterium extorquens* (Integrated Genomics, accession RMQ07946), and the anaerobic phototrophic bacteria *R. sulfidophilum* (accession AAF99437, *39*) and *Rhodopseudomonas palustris* (accession CAE29904, *40*; data not shown). Alignments of the primary structure of SoxD of *P. pantotrophus* with the amino acid sequences deduced from the newly available *soxD* genes suggested a His/Met axial coordination of the heme-1 iron by His-74 of the CysAlaSerCysHis motif and an invariant Met-121. A novel ProCysMetXaaAspCys motif is located downstream of the heme-binding motif of $SoxD_1$ and SoxD from other chemo- and phototrophic sulfur bacteria (Figure 2). The three sulfur amino acids within five invariant amino acid residues in this motif suggest a role in the unique reaction mechanism of sulfur dehydrogenase, thus possibly indicating the significance of this cytochrome as a heme enzyme rather than an electron mediator.

Analysis of the intervening sequence of SoxD of *P. pantotrophus* from amino acid 240−279 exhibited some signal peptide characteristics and suggested a peptidase cleavage site before Ala-274, consistent with the −3, −1 rule (*41*, *42*).

Isolation of SoxCD₁ and SoxD₂ from P. pantotrophus GB17. Sox proteins that reconstitute the sulfur-oxidizing enzyme system of *P. pantotrophus* were routinely purified with 2 μM phenylmethylsulfonyl fluoride (PMSF),[1] 2 mM sodium thiosulfate, and 1 mM magnesium sulfate added to the buffers for column chromatography. Omission of the additives during the chromatographic steps finally resulted in the specific decomposition of SoxD. Sulfur dehydrogenase was eluted in one fraction after chromatography on Q-Sepharose and Sephacryl S-200 HR. However, the final chromatographic step with Resource Q separated two chromogenic fractions at 0 and 0.3 M sodium chloride. The 0 M NaCl fraction contained a major protein of about 13 kDa as determined by SDS−PAGE, while the 0.3 M NaCl fraction contained proteins of 13, 26−30, and 47 kDa (Figure 3).

The subunits of sulfur dehydrogenase as purified with stabilizing additives in the buffer are clearly separated from SDS−PAGE at 43 kDa (SoxC) and 47 kDa (SoxD) (Figure 4A; *14*). Without additives, SoxD is not present at 47 kDa; instead, faint bands appear at 30 and 26 kDa in Coomassie stain (Figure 4A). Antibodies against $OP\text{-}D_1$ identified the heme-1 domain of sulfur dehydrogenase isolated in the presence of additives in the major 47- and minor 30- and

[1] Abbreviations: PMSF, phenylmethylsulfonyl fluoride.

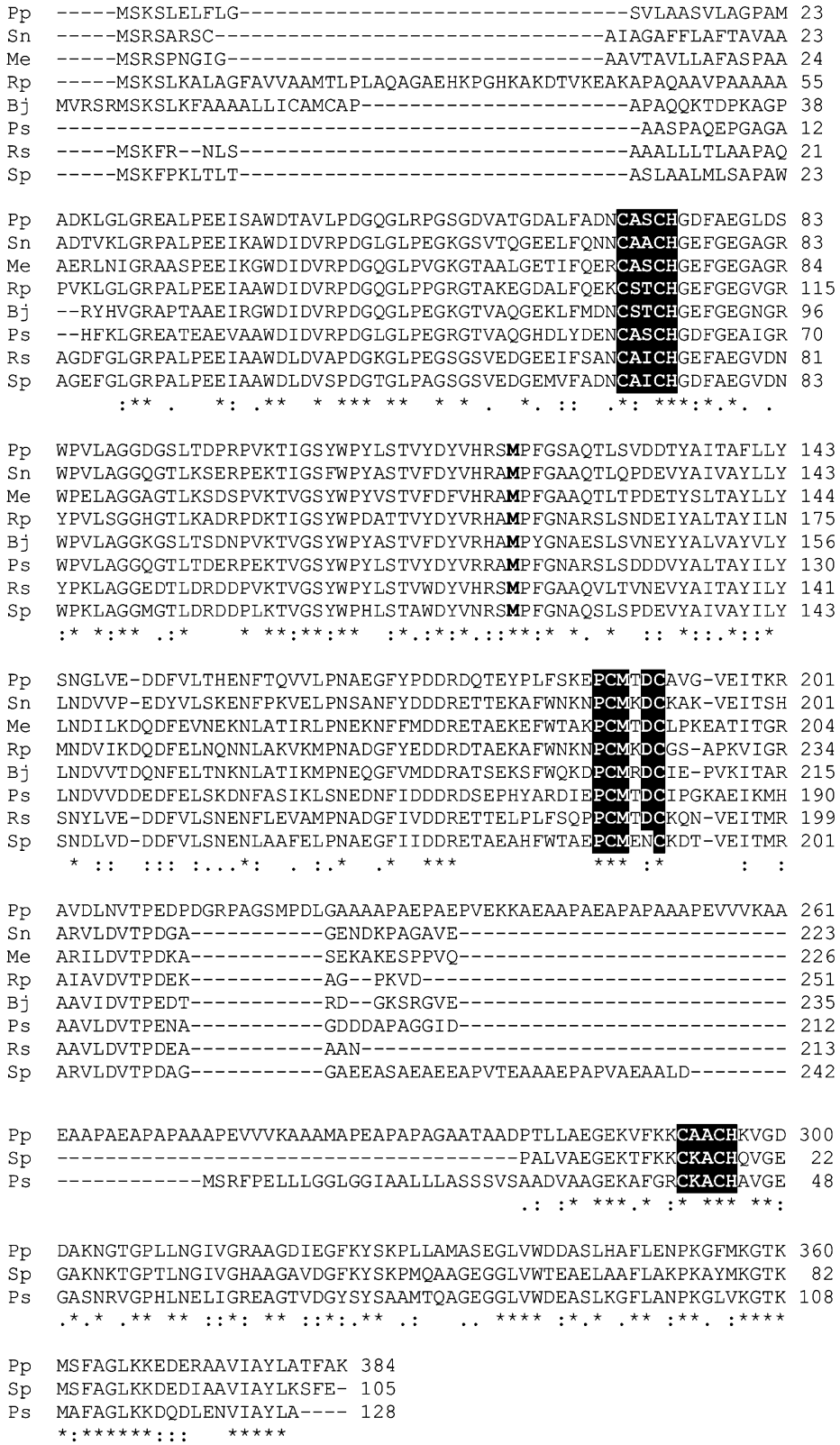

FIGURE 2: Alignment of SoxD homologous proteins. The symbols indicate identical (*), conserved (:), and semiconserved (.) residues in all sequences. The heme motifs and the PCMXDC motifs are highlighted in black. The invariant methionine residues are indicated by bold characters. Pp, *Paracoccus pantotrophus*; Sn, *Starkeya novella*; Me, *Methylobacterium extorquens*; Rp, *Rhodopseudomonas palustris;* Bj, *Bradyrhizobium japonicum*; Ps, *Pseudaminobacter salicylatoxidans* KCT001; Rs, *Rhodovulum sulfidophilum*; Sp, *Silicibacter pomeroyi*.

26-kDa polypeptides. Without additives, the 47-kDa band was not present, while the 30- and 26-kDa polypetides appeared at significantly increased intensity (Figure 4B), suggesting decomposition of SoxD which, however, preserved the heme-1 domain. No signal was observed from the 0 M NaCl fraction of the Resource Q eluate with OP-D_1 (Figure 4B) and OP-C antibodies (Figure 4C). Specific antibodies against SoxC and the heme-1 and heme-2 domains of SoxD were used to assign the different polypeptides separated by SDS−PAGE. OP-C antibodies identified the

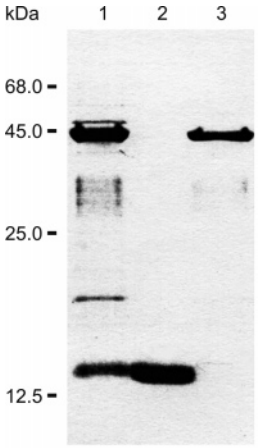

FIGURE 3: Decomposition of sulfur dehydrogenase purified without stabilizing additives. Proteins were separated by SDS−PAGE. Samples (2 μg of protein) from pool fractions of column eluates were applied to each well and stained with Coomassie blue. Lane 1, Sephacryl S-200 HR pool; lane 2, Resource Q 0 M NaCl pool; lane 3, Resource Q 0.3 M NaCl pool.

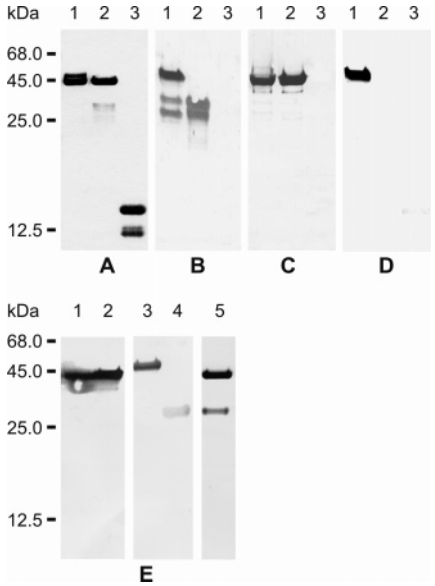

FIGURE 4: SDS−PAGE of sulfur dehydrogenase of strain GB17 purified with and without additives (A−D) and of strain GB*soxF*Δ (E). To each lane, 2 μg of protein was applied. Lane 1, Sox(CD)$_2$ purified with 2 μM PMSF, 2 mM thiosulfate, and 1 mM magnesium sulfate; lane 2, SoxCD$_1$ isolated without the additives; lane 3, SoxD$_2$ isolated without the additives. (A) Coomassie stain. (B) Western blot using OP-D$_1$ antibodies for detection of the heme-1 domain. (C) Western blot using OP-C antibodies for detection of SoxC. (D) Western blot using OP-D$_2$ antibodies for detection of the heme-2 domain. (E) SoxCD$_{F\Delta}$ of strain GB*soxF*Δ; Lanes 1 and 2, Western blot using OP-C antibodies; lane 1, Sox(CD)$_2$ of strain GB17; lane 2, SoxCD$_{F\Delta}$ of GB*soxF*Δ. Lanes 3 and 4, Western blot using OP-D$_2$ antibodies; lane 3, Sox(CD)$_2$ of strain GB17; lane 4, SoxCD$_{F\Delta}$ of GB*soxF*Δ; lane 5, Coomassie stain of SoxCD$_{F\Delta}$ of GB*soxF*Δ.

43-kDa polypeptide as SoxC, and the immunoblots of sulfur dehydrogenase purified either with or without stabilizing additives appeared to be similar (Figure 4C). OP-D$_2$ antibodies detected the heme-2 domain SoxD of sulfur dehydrogenase isolated with additives but not without (Figure 4D). However, OP-D$_2$ antibodies identified the 13-kDa polypeptide as the heme-2 domain of the SoxD, designated SoxD$_2$ (Figure 4D).

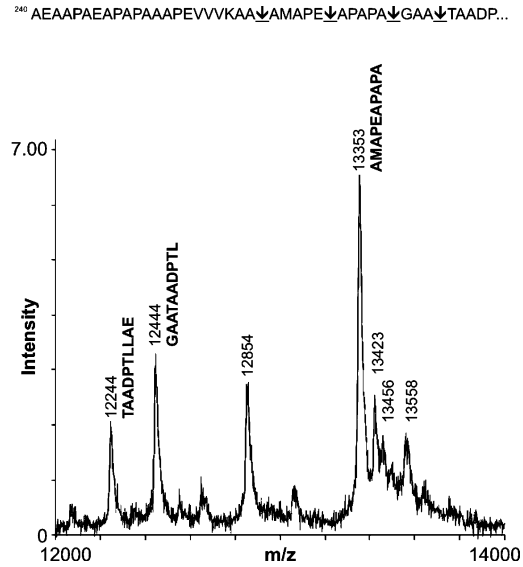

FIGURE 5: MALDI mass spectrometry of SoxD$_2$. Homogeneous SoxD$_2$ (1 μL of 26.3 μM) was added to 9 μL of a solution containing saturated sinapic acid in 50% (v/v) trifluoroacetic acid (0.1%) and 50% (v/v) acetonitrile, subjected to a MALDI slide and dried prior to analysis. The insets indicate the amino acid sequence as determined by automated Edman degradation of the respective peaks. The upper inset shows a partial intervening amino acid sequence between the heme 1 and heme 2 domain of SoxD with verified peptidase cleavage sites (indicated by arrows).

MALDI mass spectrometry of SoxD$_2$ revealed masses of 12 244, 12 444, 12 854, and 13 353 Da (Figure 5). To assign these masses, the N-terminal amino acid sequences of the different polypeptides of the SoxD$_2$ fraction of the Resource Q chromatography were determined. The sequence TAADPTLLAE was determined from the 12 244-Da polypeptide; GAATAADPTI, from the 12 444-Da polypeptide; and AMAPEAPAPA, from the 13 353-Da polypeptide. The theoretical masses of the respective SoxD$_2$ polypeptides were 11 604, 11 804, and 12 711, respectively, suggesting masses of 639.6, 640.4, and 642.3 for the heme moiety. The mass of the 12 854-Da polypeptide (Figure 5) without heme (12 214 Da) was close to that of a polypeptide with ^{266}A as the N terminus (12 221 Da). The different N termini of SoxD$_2$ suggested a corresponding population of C termini for SoxD$_1$, which varied by at most 13 amino acids.

The molecular mass of sulfur dehydrogenase purified in the presence of additives by DGGE was 180 kDa (Figure 6), confirming the $\alpha_2\beta_2$ heterotetrameric structure of Sox(CD)$_2$ reported previously (*14*). DGGE of sulfur dehydrogenase as purified without additives was homogeneous as judged by SDS−PAGE (Figure 4A) and revealed three bands of masses around 70 kDa (Figure 6), suggesting an $\alpha\beta$ heterodimeric structure possibly present as different confomers of SoxCD$_1$.

The heme content as determined by hemochrome analysis (*20*) of the homogeneous protein preparations was 3.65 mol of heme [mol of Sox(CD)$_2$]$^{-1}$, 1.08 mol of heme [mol of SoxCD$_1$]$^{-1}$, 0.80 mol of heme [mol of SoxD$_2$]$^{-1}$, and 0.76 mol of heme [mol of horse cytochrome *c*]$^{-1}$. These data matched well with the heme content expected from the primary and quaternary structures.

When these data are taken together, upon purification of Sox(CD)$_2$ without addition of a protease inhibitior and other additives, the cytochrome subunit SoxD was cleaved at

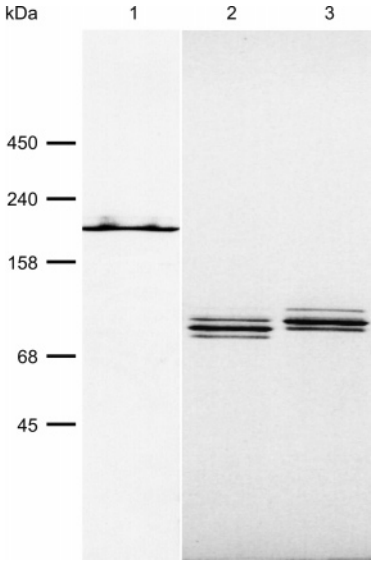

FIGURE 6: Native molecular mass of $Sox(CD)_2$ and $SoxCD_1$ by DGGE. Sulfur dehydrogenase complex of the wild-type isolated with (lane 1) and without (lane 2) additives. Sulfur dehydrogenase of strain GBΩX(pVKP6; pRI*soxCD1*) isolated with additives (lane 3). A total of 2 μg of protein was applied to each well.

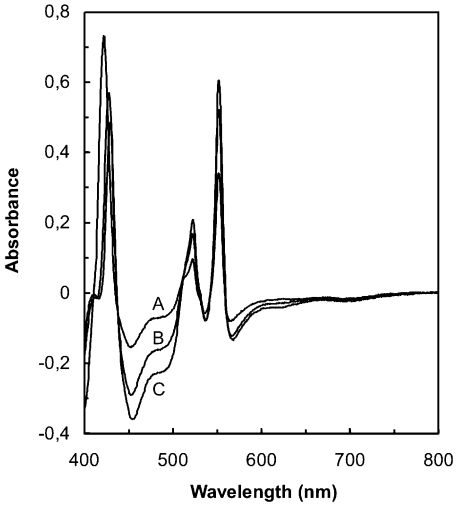

FIGURE 7: Air-oxidized minus dithionite-reduced difference spectra of $Sox(CD)_2$, $SoxCD_1$, and $SoxD_2$. (A) 0.35 mg mL^{-1} $SoxD_2$. (B) 2.5 mg mL^{-1} $Sox(CD)_2$. (C) 2.2 mg mL^{-1} $SoxCD_1$.

various sites in an intervening amino acid sequence to yield the $\alpha\beta$ heterodimeric complex $SoxCD_1$ and $SoxD_2$. Thus, the heme-2 domain appeared to be required for formation of the tetrameric structure of sulfur dehydrogenase.

UV−Vis Spectroscopy of SoxCD1 and SoxD2. The electronic absorption spectra of air-oxidized and dithionite-reduced $Sox(CD)_2$, $SoxCD_1$, and $SoxD_2$ were characteristic for proteins with *c*-type hemes. The dithionite-reduced minus air-oxidized difference spectrum of $Sox(CD)_2$ (Figure 7) exhibited identical absorption features as described previously with maxima at 427.5, 522, and 552 nm (*14*). The difference spectrum of $SoxCD_1$ showed maxima at 410, 429.5, 522.5, and 552 nm (Figure 7). The difference spectrum of the isolated $SoxD_2$ carrying the heme-2 domain of SoxD showed a Soret maximum shifted to 422 nm and otherwise identical characteristics as the complexes $Sox(CD)_2$ and $SoxCD_1$ (Figure 7). The molar extinction coefficient ϵ of $Sox(CD)_2$ was 73.8 cm^2 μmol^{-1}, 21.1 cm^2 μmol^{-1} for $SoxCD_1$, and 17.8 cm^2 μmol^{-1} for $SoxD_2$, respectively. These molar extinction coefficients reflected the heme content of the respective subunit together with the quaternary structure of sulfur dehydrogenase.

Table 2: Catalytic Properties of the Sulfur Dehydrogenases $Sox(CD)_2$ and $SoxCD_1$

SoxCD species in assay mixture[a]	cytochrome *c* reduction rate (mU)			yield of electrons (mol of cytochrome *c* reduced/mol of thiosulfate)
	hydrogen sulfide	thiosulfate	sulfite	
$Sox(CD)_2$[b]	5.1	4.2	3.2	7.9
$Sox(CD)_2$[c]	5.9	4.3	3.0	7.8
$SoxCD_{F\Delta}$	5.1	3.9	2.9	8.2
$SoxCD_1$[d]	6.6	4.4	2.7	6.8
$SoxCD_1$[e]	5.8	5.4	2.7	8.4
none	1.6	1.4	1.2	2.5

[a] The assays contained 0.5 nmol/mL of each SoxYZ, SoxB, and SoxXA of the identical preparation and concentrations of the sulfur substrates as specified in the Materials and Methods. [b] 0.5 nmol/mL $Sox(CD)_2$ of strain GB17. [c] 0.5 nmol/mL $Sox(CD)_2$ of strain GBΩX(pVKB9). [d] 1.0 nmol/mL $SoxCD_1$ of strain GBΩX(pVKP6; pRI*soxCD1*). [e] 1.0 nmol/mL $SoxCD_1$ purified from strain GB17 without stabilizing additives.

Catalytic Properties of SoxCD1. The sulfur-oxidizing enzyme system of *P. pantotrophus* reconstituted from $Sox(CD)_2$, SoxYZ, SoxXA, and SoxB accepts hydrogen sulfide, sulfur, thiosulfate, and sulfite for reduction of horse cytochrome *c* (*1*). Using $SoxCD_1$ of *P. pantotrophus* for reconstitution of the Sox system, this system was equally active with respect to the substrates examined, like hydrogen sulfide, thiosulfate, and sulfite, the rate of activity, and reactivity with these substrates (Table 2). Moreover, as expected from the theoretical yield of electrons, with $SoxCD_1$, the Sox system yielded about eight electrons per mole of thiosulfate (Table 2). Thus, with $SoxCD_1$, the reconstituted Sox system was identically efficient as complemented with the same amount of protein of $Sox(CD)_2$. These data suggested that exclusively the heme-1 domain of SoxD was required for activity, substrate specificity, and electron yield of the sulfur-oxidizing system.

Kinetic data were determined for the Sox enzyme system reconstituted either with $Sox(CD)_2$ or $SoxCD_1$ and sodium sulfide, thiosulfate, and sulfite as the substrates. The enzyme activities were performed with excess horse cytochrome *c* and limiting concentrations of sodium sulfide, thiosulfate, and sulfite, respectively. From the experiments, the Michaelis constants, K_m, were determined by fitting the standard Michaelis−Menten equation in its integrated form, measuring concentration−time data by nonlinear regression. Standard deviations were also calculated for the evaluated kinetic constants. With $Sox(CD)_2$, the K_m for sulfide was 1.2 μM; for thiosulfate, 2.3 μM; and for sulfite, 2.6 μM, while k_{cat} ranged from 0.19−0.15 s^{-1}. With $SoxCD_1$, the K_m values for sulfide, thiosulfate, and sulfite were 3.7, 2.8, and 1.9 μM, respectively, and the respective k_{cat} values ranged from 0.28 to 0.11 s^{-1} (Table 3). These data demonstrated that the kinetic properties of the heterodimeric form of sulfur dehydrogenase did not significantly differ from the tetrameric form.

Electrochemical Properties of Sox(CD)2. From $Sox(CD)_2$ of *P. pantotrophus*, all hemes are redox-active within the redox step from −0.1 to 0.4 V as evident from the

Table 3: Kinetic Constants of the Sox Enzyme System Reconstituted with Tetra- or Dimeric Sulfur Dehydrogenase[a]

sulfur dehydrogenase	kinetic constant	substrate sulfide	substrate thiosulfate	substrate sulfite
$Sox(CD)_2$	K_m (μM)	1.21 ± 0.08	2.28 ± 0.12	2.55 ± 0.11
	k_{cat} (s^{-1})	0.19 ± 0.002	0.16 ± 0.001	0.14 ± 0.002
$SoxCD_1$	K_m (μM)	3.73 ± 0.40	2.81 ± 0.11	1.94 ± 0.10
	k_{cat} (s^{-1})	0.28 ± 0.01	0.17 ± 0.002	0.11 ± 0.001

[a] The assays contained 0.5 nmol/mL of each SoxYZ, SoxB, and SoxXA of the identical preparation and concentrations of the sulfur substrates as specified in the Materials and Methods, and the concentration of horse cytochrome *c* was 105 mM. $Sox(CD)_2$ or $SoxCD_1$ were added at a concentration of 0.5 nmol/mL.

electrochemically induced vis difference spectrum. Similar spectral features were obtained for $SoxCD_1$ as isolated from the wild type without stabilizing additives, while $SoxD_2$ exhibited a small shift of the Soret band to 416 nm (data not shown) as similarly observed from the electronic difference spectra.

The redox potentials of the $Sox(CD)_2$ protein from *P. pantotrophus* were monitored in the visible spectral range. The theoretical Nernst fit at 550 nm yielded a best fit for two midpoint potentials at $E_{m_1} = 218 \pm 10$ mV and $E_{m_2} = 268 \pm 10$ mV for the oxidative (●) and reductive (○) titration. The error was estimated from the standard deviation of several titrations (Figure 8A). The titrations led to a best fit with a number of transferred electrons of 0.8−0.9 as expected for a monoheme cytochrome complex and were fully reversible. No significant pH dependency was observed comparing the redox potentials as monitored for the samples equilibrated at pH 6 and 8 (data not shown). The $SoxCD_1$ and $SoxD_2$ proteins showed a redox-dependent transition at 278 ± 10 mV. The oxidative (●) and reductive (○) titration curves are shown in parts B and C of Figure 8, respectively. Interestingly, both proteins have a slightly higher potential than the complex, which does not affect the catalytic property of $SoxCD_1$.

Figure 9 shows the oxidized-minus-reduced-induced FTIR difference spectra of the $Sox(CD)_2$ protein from *P. pantotrophus* (A). Briefly, in the amide I range (1680−1620 cm^{-1}), strong signals at 1688, 1672, and 1662 cm^{-1} indicate absorbance changes of $\nu_{C=O}$ groups from the polypeptide backbone. These difference signals are caused by small alterations in the structure upon the redox process. In the spectral region from 1560 to 1520 cm^{-1} (the amide II range), contributions from coupled CN-stretching and NH-bending modes are seen at 1568 and 1542 cm^{-1}. In addition to amide II signals, vibrational modes from aromatic amino acid side chains and heme C═C groups will contribute, as well as antisymmetric $\delta(COO)^-$ modes caused by protonation/deprotonation of COOH groups. The vibrational modes for the heme centers can be typically found in the full mid-infrared range, involving the ring vibration of the C−C and C−N modes as found previously from cytochrome *c* and the latter from several other heme proteins (*43*, *44*).

The direct comparison of the oxidized-minus-reduced FTIR difference spectra with $SoxCD_1$ (B) and $SoxD_2$ (C) indicates that the redox-induced difference spectrum of the complete $Sox(CD)_2$ protein is dominated by the reorganization of the heme-1 domain (Figure 9B). Interestingly, a signal can be observed at a position characteristic for protonated

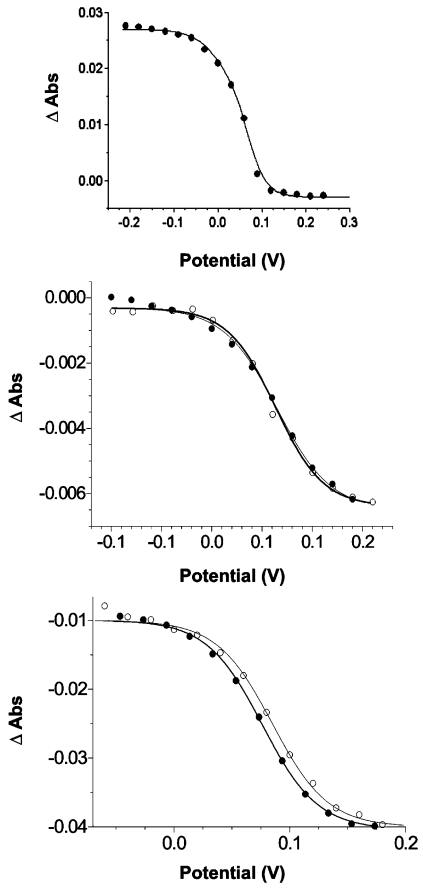

FIGURE 8: Oxidative (●) and reductive (○) potential titrations of sulfur dehydrogenase and $SoxD_2$ of *P. pantotrophus* fitted at 550 nm. (A) $Sox(CD)_2$ with midpoint potentials $E_{m_1} = 218 \pm 10$ mV and $E_{m_2} = 268 \pm 10$ mV. (B) $SoxD_2$ with a midpoint potential of E_m 278 ± 10 mV. (C) $SoxCD_1$ with a midpoint potential of $E_m = 278 \pm 10$ mV.

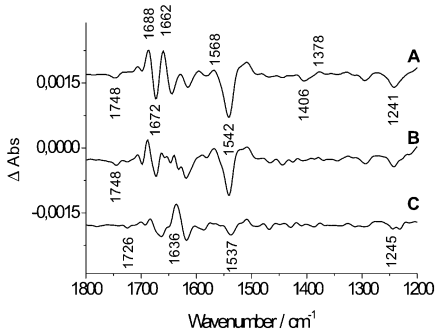

FIGURE 9: Oxidized-minus-reduced FTIR difference spectra of sulfur dehydrogenase and $SoxD_2$ of *P. pantotrophus* GB17. (A) $Sox(CD)_2$. (B) $SoxCD_1$. (C) $SoxD_2$.

aspartic or glutamic acid side chains (*45*, *46*). This negative feature at 1748 cm^{-1} indicates the protonation of an acidic residue with the reduction of the enzyme. This signal is present for the full complex, except for $SoxD_2$, pointing to a residue in the vicinity of the heme-1-binding site. An invariant aspartate is part of the novel motif in the heme-1 domain and possibly involved in the reaction mechanism.

Function of the Heme-2 Domain of SoxD. The heme-2 domain of SoxD, $SoxD_2$, was not required for catalytic activity *in vitro* and appeared to be crucial for formation of the $\alpha_2\beta_2$ quaternary structure of sulfur dehydrogenase. The latter property did not allow conclusions on the function of

$SoxD_2$ in electron transfer to the cytoplasmic membrane or to molecular oxygen. *P. pantotrophus* is obligately aerobic, while other sulfur-oxidizing bacteria are anaerobic phototrophic or microaerophilic.

The homogenote mutant GB*soxF*Δ grows chemotrophically with thiosulfate albeit with a doubling time of 11 h, while the wild-type grows with about 6 h (data not shown). Re-examination of the mutant GB*soxF*Δ uncovered an additional guanidine nucleotide at position 3492 (accession X79242 PDSOX) leading to a frame-shift mutation in *soxD* after Gly^{337} and a stop codon after 33 amino acids. Thus, $SoxD_{F\Delta}$ of the the sulfur dehydrogenase complex of strain GB*soxF*Δ contained only 370 amino acids, with the last 33 changed to AGLGRCIAARLPGKPOGFHEGHQDVLCRAEERG. This mutation eliminated the immunogenic epitope at the carboxy-terminal end for OP-D_2 antibodies but did not alter the catalytic activity *in vitro* as compared to $Sox(CD)_2$ of the wild type (Table 2). However, the mutation led to the digestion of the complete heme-2 domain and yielded a SoxD1 of 30 kDa (Figure 4E). The molecular mass as determined by native DGGE revealed 70 kDa (data not shown), suggesting a dimeric structure designated $SoxCD_{F\Delta}$.

To examine the physiological significance of the heme-2 domain with respect to aerobic sulfur oxidation, a mutant was constructed expressing $soxD_1$ but not $soxD_2$. Such a mutation would result in a $SoxD_1$ species with a distinct C terminus rather than different C termini as suggested for the enzyme isolated without additives.

As a background for expression of $soxD_1$, the homogenote strain, *P. pantotrophus* GBΩX, was constructed and unable to express the *sox* structural genes (see the Materials and Methods and Table 1), and this strain was used for complementation analysis. Plasmid pVKB9 (*1*) was conjugated into strain GBΩX. The resulting strain GBΩX(pVKB9) expressed the complete set of the *sox* structural genes and formed $Sox(CD)_2$. Whole cells and cell-free extracts of GBΩX(pVKB9) were identically active as the wild-type strain GB17 when thiosulfate was included to the medium to induce the *sox* genes (data not shown). For formation of $SoxCD_1$, two plasmids were constructed (i) pVKP6, which carried the *soxVWXYZAB* but not the *soxCD* genes, and (ii) pRI$soxCD_1$ with *soxC* and the truncated $soxD_1$ gene, with a stop codon introduced after Ala^{261}, encoding a matured $SoxD_1$ of 237 amino acids with a theoretical molecular mass of the polypeptide of 24 947 Da, excluding the heme.

The specific thiosulfate-dependent oxygen uptake rate of the wild-type *P. pantotrophus* GB17 grown in the presence of thiosulfate was 0.39 μmol of oxygen min^{-1} (mg of protein)$^{-1}$, while strain GBΩX(pVKP6) did not oxidize thiosulfate. However, when this strain was further complemented with pRI$soxCD_1$ cells of strain GBΩX(pVKP6; pRI$soxCD_1$) regained thiosulfate-oxidizing ability albeit at about 40% of the specific oxygen consumption rate of the wild type. Strain GBΩX(pVKP6; pRI$soxCD_1$) consumed about 3.3 mol of oxygen atoms/mol of thiosulfate, which was identical to that of the wild type (Table 4) and about 75% of the theoretical yield. *Paracoccus* strains utilize about 75% of the substrate at a rapid rate and thereafter at a significantly decreased rate (*18*).

The thiosulfate-dependent cytochrome *c* reduction rates and yields in electrons from cell-free extracts were similar to those of whole cells of strain GBΩX(pVKP6; pRI$soxCD_1$) as compared to the wild-type GB17. Cells of strain GBΩX(pVKP6) did not oxidize thiosulfate, as similarly observed from homogenote mutants with a deletion in *soxC* and rendering sulfur dehydrogenase nonfunctional (*15*). However, cell-free extracts of strain GBΩX(pVKP6) were about identically active as extracts of strain GBΩX(pVKP6; pRI$soxCD_1$), and both strains exhibited 55% of the activity of the wild type. The yield of electrons of extracts of strain GBΩX(pVKP6) was only about 2 mol of electrons/mol of thiosulfate, while strain GBΩX(pVKP6; pRI$soxCD_1$) yielded 6 electrons/mol of thiosulfate. The significant difference upon the introduction of the $soxCD_1$ genes into GBΩX(pVKP6) was, therefore, the increase in electron yield to the wild-type level (Table 4). This result demonstrated that the heme-1 domain was sufficient for the function of sulfur dehydrogenase *in vivo* and *in vitro*.

Table 4: Thiosulfate Oxidations Rates and Efficiencies of Whole Cells and Cell-Free Extracts of *P. pantotrophus* Strains Complemented for Sulfur Dehydrogenase[a]

	specific thiosulfate oxidation rate			
	whole cells		cell-free extract	
strain	specific activity [μmol of O_2 min^{-1} (mg of protein)$^{-1}$]	yield (mol of oxygen atom mol of thiosulfate^{-1})	specific activity (mU)	yield (mol of electrons mol of thiosulfate^{-1})
GB17	0.39	3.7	5.6	6.5
GBΩX	0	0	0	0
GBΩX(pVKB9)	0.37	3.7	1.4	6.1
GBΩX(pVKP6)	0	0	3.1	2.6
GBΩX(pVKP6; pRI$soxCD_1$)	0.15	3.3	2.8	6.0

[a] The assay (3.0 mL) for thiosulfate oxidizing activity contained 10 mg of protein of whole cells and was determined with a polarographic oxygen electrode as described (*15*). The thiosulfate-dependent cytochrome-*c*-reducing activity of the A65 fraction was determined in the assay described in the Materials and Methods with 10 mg of protein instead of the addition of the homogeneous Sox proteins.

The Sox enzyme system of *P. pantotrophus* reconstituted from homogeneous proteins SoxXA, SoxYZ, SoxB and sulfur dehydrogenase either as $Sox(CD)_2$ or $SoxCD_1$ transfers eight electrons from thiosulfate to horse cytochrome *c* and with omission of sulfur dehydrogenase at a reduced rate and yield of only about two electrons (Table 2). Therefore, the lower activity and the yield of 2 mol of electrons/mol of thiosulfate oxidized by cell-free extracts of GBΩX(pVKP6) is in accordance with the relative activity and electron yield of the reconstituted enzyme system.

CONCLUSIONS

SoxD of *P. pantotrophus* is a hybrid *c*-type cytochrome with a heme-1 and heme-2 domain similarly present only in two other chemotrophic bacterium, while SoxD of anaerobic phototrophic sulfur-oxidizing bacteria contain the heme-1 domain. The heme-1 domain of SoxD of *P. pantotrophus* is required for full catalytic activity of sulfur dehydrogenase, electron yield, and transfer of electrons to the cytoplasmic membrane to enable *P. pantotrophus* to use molecular oxygen as a final electron acceptor for aerobic sulfur oxidation. The heme-2 domain is dispensable for catalytic

activity but causes complexation of the subunits to the tetrameric structure of sulfur dehydrogenase. Thus far, no data are available on the quaternary structure of sulfur dehydrogenases from other sources. This is the first report that the deletion of a complete heme domain did not alter the catalytic but the structural properties of an enzyme.

ACKNOWLEDGMENT

We thank Rolf Wichmann for the calculation of the enzymic constants by nonlinear regression analysis and Bettina Höller, Josefina Ringk, Sabine Vogt, and Monique van Straaten for expert technical assistance.

REFERENCES

1. Rother, D., Henrich, H.-J., Quentmeier, A., Bardischewsky, F., and Friedrich, C. G. (2001) Novel genes of *sox* gene cluster, mutagenesis of the flavoprotein SoxF, and evidence for a general sulfur oxidizing system in *Paracoccus pantotrophus* GB17, *J. Bacteriol. 183*, 4499−4508.
2. Trüper, H.-G., and Fischer, U. (1982) Anaerobic oxidation of sulfur compounds as electron donors for bacterial photosynthesis, *Philos. Trans. R. Soc. London. 298*, 529−542.
3. Brune, D. C. (1989) Sulfur oxidation by phototrophic bacteria, *Biochim. Biophys. Acta 975*, 189−221.
4. Takakuwa, S. (1992) Biochemical aspects of microbial oxidation of inorganic sulfur compounds, in *Organic Sulfur Chemistry. Biochemical Aspects* (Oae, S., and Okuyama, T., Eds.) pp 1−43, CRC Press, Boca Raton, FL.
5. Nelson, D. C., and Fisher, C. R. (1995) Chemoautotrophic and methanotrophic endosymbiotic bacteria at deep-sea vents and seeps, in *The Microbiology of Deep-Sea Hydrothermal Vents* (Karl, D. M., Ed.) pp 125−167, CRC Press, Boca Raton, FL.
6. de Zwart, J. M. M., Nelisse, P. N., and Kuenen, J. G. (1996) Isolation and characterization of *Methylophaga sulfidovorans*, sp. nov.: An obligately methylotrophic, aerobic, dimethyl sulfide oxidizing bacterium from a microbial mat, *FEMS Microbiol. Ecol. 20*, 261−270.
7. Kelly, D. P., Shergill, J. K., Lu, W.-P., and Wood, A. P. (1997) Oxidative metabolism of inorganic sulfur compounds by bacteria, *Antonie van Leeuwenhoek 71*, 95−107.
8. Friedrich, C. G., Rother, D., Bardischewsky, F., Quentmeier, A., and Fischer, J. (2001) Oxidation of inorganic sulfur compounds by bacteria: Emergence of a common mechanism? *Appl. Environ. Microbiol. 67*, 2873−2882.
9. Robertson, L. A., and Kuenen, J. G. (1983) *Thiosphaera pantotropha* gen. nov. sp. nov., a facultatively anaerobic, facultative autotrophic sulphur bacterium, *J. Gen. Microbiol. 129*, 2847−2855.
10. Rainey, F. A., Kelly, D. P., Stackebrandt, E., Burghardt, J., Hiraishi, A., Katayama, Y., and Wood, A. P. (1999) A re-evaluation of the taxonomy of *Paracoccus denitrificans* and a proposal for the combination *Paracoccus pantotrophus* comb. nov., *Int. J. Syst. Bacteriol. 49*, 645−651.
11. Friedrich, C. G., Quentmeier, A., Bardischewsky, F., Rother, D., Kraft, R., Kostka, S., and Prinz, H. (2000) Novel genes coding for lithotrophic sulfur oxidation of *Paracoccus pantotrophus* GB17, *J. Bacteriol. 182*, 4677−4687.
12. Bamford, V. A., Bruno, S., Rasmussen, T., Appia-Ayme, C., Cheesman, M. R., Berks, B. C., and Hemmings, A. M. (2002) Structural basis for the oxidation of thiosulfate by a sulfur cycle enzyme, *EMBO J. 21*, 5599−5610.
13. Quentmeier, A., and Friedrich, C. G. (2001) The cysteine residue of the SoxY protein as the active site of protein-bound sulfur oxidation of *Paracoccus pantotrophus* GB17, *FEBS Lett. 503*, 168−172.
14. Quentmeier, A., Kraft, R., Kostka, S., Klockenkämper, R., and Friedrich, C. G. (2000) Characterization of a new type of sulfite dehydrogenase, *Arch. Microbiol. 173*, 117−125.
15. Wodara, C., Bardischewsky, F., and Friedrich, C. G. (1997), Cloning and characterization of sulfite dehydrogenase, two *c*-type cytochromes, and a flavoprotein of *Paracoccus denitrificans* GB17: Essential role of sulfite dehydrogenase in lithotrophic sulfur oxidation, *J. Bacteriol. 179*, 5014−5023.
16. Kappler, U., and Dahl, C. (2001) Enzymology and molecular biology of prokaryotic sulfite oxidation, *FEMS Microbiol. Lett. 2003*, 1−9.
17. Kappler, U., Bennett, B., Rethmeier, J., Schwarz, G., Deutzmann, R., McEwan, A. G., and Dahl, C. (2000) Sulfite:cytochrome *c* oxidoreductase from *Thiobacillus novellus*. Purification, characterization, and molecular biology of a heterodimeric member of the sulfite oxidase family, *J. Biol. Chem. 275*, 13202−13212.
18. Friedrich, C. G., and Mitrenga, G. (1981) Oxidation of thiosulfate by *Paracoccus denitrificans* and other hydrogen bacteria, *FEMS Microbiol. Lett. 10*, 208−210.
19. Friedrich, C. G., Meyer, O., and Chandra, T. S. (1986) Molybdenum-dependent sulfur oxidation in facultatively lithoautotrophic thiobacteria, *FEMS Microbiol. Lett. 37*, 105−108.
20. Berry, E. A., and Trumpower, B. L. (1987) Simultaneous determination of hemes *a*, *b*, and *c* from pyridine hemochrome spectra, *Anal. Biochem. 161*, 1−15.
21. Hellwig, P., Behr, J., Ostermeier, C., Richter, O.-M. H., Pfitzner, U., Odenwald, A., Ludwig, B., Michel, H., and Mäntele, W. (1998) Involvement of glutamic acid 278 in the redox reaction of the cytochrome *c* oxidase from *Paracoccus denitrificans* investigated by FTIR spectroscopy, *Biochemistry 37*, 7390−7399.
22. Hellwig, P., Scheide, D., Bungert, S., Mäntele, W., and Friedrich, T. (2000) FT-IR spectroscopic characterization of NADH:ubiquinone oxidoreductase (complex I) from *Escherichia coli*: Oxidation of FeS cluster N2 is coupled with the protonation of an aspartate or glutamate side chain, *Biochemistry 39*, 10884−10891.
23. Laemmli, U. K. (1970) Cleavage of structural proteins during the assembly of the head of bacteriophage T4, *Nature 227*, 680−685.
24. Andersson, L. O., Borg, H., and Mikaelsson, M. (1972) Molecular weight estimations of proteins by electrophoresis in polyacrylamide gels of graded porosity, *FEBS Lett. 20*, 199−202.
25. Weber, K., Pringle, J. R., and Osborn, M. (1972) Measurements of the molecular weights by electrophoresis on SDS polyacrylamide gels, *Methods Enzymol. 26*, 3−27.
26. Fischer, J., Quentmeier, A., Kostka, S., Kraft, R., and Friedrich, C. G. (1996) Purification and characterization of the hydrogenase from *Thiobacillus ferrooxidans*, *Arch. Microbiol. 165*, 289−296.
27. Towbin, H., Staehelin, T., and Gordon, J. (1979) Electrophoretic transfer of proteins from polyacrylamide gels to nitrocellulose sheets: Procedure and some applications, *Proc. Natl. Acad. Sci. U.S.A. 76*, 4350−4354.
28. Bradford, M. M. (1976) A rapid and sensitive method for the quantitation of microgram quantities of protein utilizing the principle of protein-dye binding, *Anal. Biochem. 72*, 248−254.
29. Sambrook, J., Maniatis, T., and Fritsch, E. F. (1989) *Molecular Cloning: A Laboratory Manual*, 2nd ed., Cold Spring Harbor Laboratory, Cold Spring Harbor, New York.
30. Kieser, T. (1984) Factors affecting the isolation of CCC DNA from *Streptomyces lividans* and *Escherichia coli*, *Plasmid 12*, 19−36.
31. Ausubel, F. M., Brent, R., Kingston, R. E., Moore, D. D., Seidman, J. G., Smith, J. A., and Struhl, K. (1994) *Current Protocols in Molecular Biology*, Wiley and Sons, New York.
32. Rémy, F., Frey, J., and Krisch, H. (1987) Interposon mutagenesis of soil and water bacteria: A family of DNA fragments designed for *in vitro* insertional mutagenesis of Gram-negative bacteria, *Gene 52*, 147−154.
33. Bardischewsky, F., and Friedrich, C. G. (2001) The *shxVW* locus is essential for oxidation of inorganic sulfur and molecular hydrogen by *Paracoccus pantotrophus* GB17: A novel function for lithotrophy, *FEMS Microbiol. Lett. 202*, 215−220.
34. Simon, R., Priefer, U., and Pühler, A. (1983) A broad host range mobilization system for *in vivo* genetic engineering: Transposon mutagenesis in Gram-negative bacteria. *Biotechnology 1*, 784−790.
35. Pfitzner U., Odenwald, A., Ostermann, T., Weingard, L., Ludwig, B., and Richter, O. M. (1998) Cytochrome *c* oxidase (heme aa_3) from *Paracoccus denitrificans*: Analysis of mutations in putative proton channels of subunit I, *J. Bioenerg. Biomembr. 30*, 89−97.
36. Altenbuchner, J., Viell, P., and Pelletier, L. (1992) Positive selection vectors based on palindromic DNA sequences, *Methods Enzymol. 216*, 457−466.
37. Vieira, J., and Messing, J. (1982) The pUC plasmid: An M13mp7-derived system for insertion mutagenesis and sequencing with synthetic universal primers, *Gene 19*, 259−268.

38. Kaneko, T., Nakamura, Y., Sato, S., Minamisawa, K., Uchiumi, T., Sasamoto, S., Watanabe, A., Idesawa, K., Iriguchi, M., Kawashima, K., Kohara, M., Matsumoto, M., Shimpo, S., Tsuruoka, H., Wada, T., Yamada, M., and Tabata, S. (2003) Complete genomic sequence of nitrogen-fixing symbiotic bacterium *Bradyrhizobium japonicum* USDA110, *DNA Res. 9*, 189−197.
39. Appia-Ayme, C., Little, P. J., Matsumoto, Y., Leech, A. P., and Berks, B. C. (2001) Cytochrome complex essential for photosynthetic oxidation of both thiosulfate and sulfide in *Rhodovulum sulfidophilum*, *J. Bacteriol. 183*, 6107−6118.
40. Larimer, F. W., Chain, P., Hauser, L., Lamerdin, J., Malfatti, S., Do, L., Land, M. L., Pelletier, D. A., Beatty, J. T., Lang, A. S., Tabita, F. R., Gibson, J. L., Hanson, T. E., Bobst, C., Torres, J. L., Peres, C., Harrison, F. H., Gibson, J., Harwood, C. S. (2004) Complete genome sequence of the metabolically versatile photosynthetic bacterium *Rhodopseudomonas palustris*, *Nat. Biotechnol. 22*, 55−61.
41. von Heijne, G. (1988) Transcending the impenetrable: How proteins come to terms with membranes, *Biochim. Biophys. Acta 947*, 307−333.
42. Wodara, C. (1995) Molekulare Analyse der Schwefel-Oxidation kodierenden DNA-Region von *Paracoccus denitrificans* GB17, Ph.D. Thesis, University of Dortmund, Germany.
43. Moss, D., Nabedryk, E., Breton, J., and Mäntele, W. (1990) Redox-linked conformational changes in proteins detected by a combination of infrared spectroscopy and protein electrochemistry. Evaluation of the technique with cytochrome *c*, *Eur. J. Biochem. 187*, 565−572.
44. Schlereth, D. D., and Mantele, W. (1993) Electrochemically induced conformational changes in cytochrome *c* monitored by Fourier transform infrared difference spectroscopy: Influence of temperature, pH, and electrode surfaces, *Biochemistry 32*, 1118−1126.
45. Siebert, F., Mäntele, W., and Kreutz, W. (1982) Evidence for the protonation of two internal carboxylic groups during the photocycle of bacteriorhodopsin: Investigation of kinetic infrared spectroscopy, *FEBS Lett. 141*, 82−87.
46. Hellwig, P., Behr, J., Ostermeier, C., Richter, O.-M. H., Pfitzner, U., Odenwald, A., Ludwig, B., Michel, H., and Mäntele, W. (1998) Involvement of glutamic acid 278 in the redox reaction of the cytochrome *c* oxidase from *Paracoccus denitrificans* investigated by FTIR spectroscopy, *Biochemistry 37*, 7390−7399.
47. Fellay, R., Frey, J., and Krisch, H. (1987) Interposon mutagenesis of soil and water bacteria: A family of DNA fragments designed for *in vitro* insertional mutagenesis of Gram-negative bacteria, *Gene 52*, 147−154.
48. Knauf, V. C., and Nester, E. W. (1982) Wide host range cloning vectors: A cosmid clone bank of an *Agrobacterium* Ti plasmid, *Plasmid 8*, 45−54.
49. Mittenhuber, G., Sonomoto, K., Egert, M., and Friedrich, C. G. (1991) Identification of the DNA region responsible for sulfur-oxidizing ability of *Thiosphaera pantotropha*, *J. Bacteriol. 173*, 7340−7344.

BI047334B